Collision Tolerant and Collision Free Packet Scheduling for Underwater Acoustic Localization

Hamid Ramezani, *Student Member, IEEE*, Fatemeh Fazel, *Member, IEEE*,
Milica Stojanovic, *Fellow, IEEE*, and Geert Leus, *Fellow, IEEE*

***Abstract*—This article considers the joint problem of packet scheduling and self-localization in an underwater acoustic sensor network with randomly distributed nodes. In terms of packet scheduling, our goal is to minimize the localization time, and to do so we consider two packet transmission schemes, namely a collision-free scheme (CFS), and a collision-tolerant scheme (CTS). The required localization time is formulated for these schemes, and through analytical results and numerical examples their performances are shown to be dependent on the circumstances. When the packet duration is short (as is the case for a localization packet), the operating area is large (above 3 km in at least one dimension), and the average probability of packet-loss is not close to zero, the collision-tolerant scheme is found to require a shorter localization time. At the same time, its implementation complexity is lower than that of the collision-free scheme, because in CTS, the anchors work independently. CTS consumes slightly more energy to make up for packet collisions, but it is shown to provide a better localization accuracy. An iterative Gauss-Newton algorithm is employed by each sensor node for self-localization, and the Cramér Rao lower bound is evaluated as a benchmark.**

***Index Terms*—Underwater acoustic networks, localization, packet scheduling, collision.**

I. Introduction

After the emergence of autonomous underwater vehicles (AUVs) in the 70s, developments in computer systems and networking have been paving a way toward fully autonomous underwater acoustic sensor networks (UASNs) [1], [2]. Modern underwater networks are expected to handle many tasks automatically. To enable applications such as tsunami monitoring, oil field inspection, bathymetry mapping, or shoreline surveillance, the sensor nodes measure various environmental parameters, encode them into data packets, and exchange the packets with other sensor nodes or send them to a fusion center. In many underwater applications, the sensed data has to be labeled with the time and the location of their origin to provide meaningful information. Therefore, sensor nodes that explore the environment and gather data have to know their position, and this makes localization an important task for the network.

Due to the challenges of underwater acoustic communications such as low data rates and long propagation delays with variable sound speed [3], a variety of localization algorithms have been introduced and analyzed in the literature [4], [5]. In contrast to underwater systems, sensor nodes in terrestrial wireless sensor networks (WSNs) can be equipped with a GPS module to determine location. GPS signals (radio-frequency signals), however, cannot propagate more than a few meters, and underwater acoustic signals are used instead. In addition, radio signals experience negligible propagation delays as compared to the sound (acoustic) waves.

An underwater sensor node can determine its location by measuring the time of flight (ToF) to several anchors with known positions, and performing multilateration. Other approaches may be employed for self-localization, such as fingerprinting [6] or angle of arrival estimation [7]. All these approaches require packet transmission from anchors.

Many factors determine the accuracy of self-localization. Other than noise, the number of anchors, their constellation and relative position of the sensor node [8], propagation losses and fading also affect the localization accuracy. Some of these parameters can be adjusted to improve the localization accuracy, but others cannot.

Although a great deal of research exists on underwater localization algorithms [1], little work has been done to determine how the anchors should transmit their packets to the sensor nodes. In long base-line (LBL) systems where transponders are fixed on the sea floor, an underwater node interrogates the transponders for round-trip delay estimation [9]. In the underwater positioning scheme of [10], a master anchor sends a beacon signal periodically, and other anchors transmit their packets in a given order after the reception of the beacon from the previous anchor. The localization algorithm in [11] addresses the problem of joint node discovery and collaborative localization without the aid of GPS. The algorithm starts with a few anchors as primary seed nodes, and as it progresses, suitable sensor nodes are converted to seed nodes to help in discovering more sensor nodes. The algorithm works by broadcasting command packets which the nodes use for time-of-flight

Manuscript received April 24, 2014; revised October 23, 2014; accepted December 29, 2014. Date of publication January 8, 2015; date of current version May 7, 2015. The research leading to these results has received funding in part from the European Commission FP7-ICT Cognitive Systems, Interaction, and Robotics under the contract #270180 (NOPTILUS), NSF Grant CNS-1212999, and ONR Grant N00014-09-1-0700. Part of this work was presented at the IEEE ICC Workshop on Advances in Network Localization and Navigation (ANLN), Sydney, Australia, June 10–14, 2014. The associate editor coordinating the review of this paper and approving it for publication was A. Zajic.

H. Ramezani and G. Leus are with the Faculty of Electrical Engineering, Mathematics and Computer Science, Delft University of Technology, 2826 CD Delft, The Netherlands (e-mail: h.mashhadiramezani@tudelft.nl; g.j.t.leus@tudelft.nl).

F. Fazel and M. Stojanovic are with the Department of Electrical and Computer Engineering, Northeastern University, MA 02611 USA (e-mail: ffazel@ece.neu.edu; millitsa@ece.neu.edu).

Color versions of one or more of the figures in this paper are available online at http://ieeexplore.ieee.org.

Digital Object Identifier 10.1109/TWC.2015.2389220

measurements. The authors evaluate the performance of the algorithm in terms of the average network set-up time and coverage. However, physical factors such as packet loss due to fading or shadowing and collisions are not included, and it is not established whether this algorithm is optimal for localization. In reactive localization [12], an underwater node initiates the process by transmitting a "hello" message to the anchors in its vicinity, and those anchors that receive the message transmit their packets. An existing medium access control (MAC) protocol may be used for packet exchanging [13]; however, there is no guarantee that it will perform satisfactorily for the localization task. The performance of localization under different MAC protocols is evaluated in [14], where it is shown that a simple carrier sense multiple access (CSMA) protocol performs better than the recently introduced underwater MAC protocols such as T-Lohi [15].

In our previous work, we considered optimal collision-free packet scheduling in a UASN for the localization task in single-channel (L-MAC) [16] and multi-channel [17] scenarios (DMC-MAC). In these algorithms, the position information of the anchors is used to minimize the localization time. In spite of the remarkable performance of L-MAC and DMC-MAC over other algorithms (or MAC protocols), they are highly demanding. The main drawback of L-MAC or DMC-MAC is that they require a fusion center which gathers the positions of all the anchors, and decides on the time of packet transmission from each anchor. In addition, these two collision-free algorithms need the anchors to be synchronized and equipped with radio modems to exchange information fast.

In this paper, we also consider packet scheduling algorithms that do not need a fusion center. Although the synchronization of the anchors which are equipped with GPS is not difficult, the proposed algorithms can work with asynchronized anchors if there is a request from a sensor node.

We assume a single-hop UASN where anchors are equipped with half-duplex acoustic modems, and can broadcast their packets based on two classes of scheduling: a collision-free scheme (CFS), where the transmitted packets never collide with each other at the receiver, and a collision-tolerant scheme (CTS), where the collision probability is controlled by the packet transmission rate in such a way that each sensor node can receive sufficiently many error-free packets for self-localization. Our contributions are listed below.

- Assuming packet loss and collisions, the localization time is formulated for each scheme, and its minimum is obtained analytically for a predetermined probability of successful localization for each sensor node. A shorter localization time allows for a more dynamic network, and leads to a better network efficiency in terms of throughput.
- It is shown how the minimum number of anchors can be determined to reach the desired probability of self-localization.
- An iterative Gauss-Newton self-localization algorithm is introduced for a sensor node which experiences packet loss or collision. Furthermore, the way in which this algorithm can be used for each packet scheduling scheme is outlined.
- The Cramér Rao lower bound (CRB) on localization is derived for each scheme. Other than the distance-dependent signal to noise ratio, the effects of packet loss due to fading or shadowing, collisions, and the probability of successful self-localization are included in this derivation.

The structure of the paper is as follows. Section II describes the system model, and outlines the self-localization process. The problem of minimizing the localization time in the collision-free and collision-tolerant packet transmission schemes is formulated and analyzed in Section III-A and Section III-B, respectively. The self-localization algorithm is introduced in Section IV. The average energy consumption is analyzed in Section V, and Section VI compares the two classes of localization packet scheduling through several numerical examples. Finally, we conclude the paper in Section VII, and outline the topics of future works.

II. System Model

We consider a UASN consisting of M sensor nodes and N anchors. The anchor index starts from 1, whereas the sensor node index starts from $N+1$. Each anchor in the network encapsulates its ID, its location, time of packet transmission, and a predetermined training sequence for the time of flight estimation. The so-obtained localization packet is broadcast to the network based on a given protocol, e.g., periodically, or upon the reception of a request from a sensor node. The system structure is specified as follows.

- Anchors and sensor nodes are equipped with half-duplex acoustic modems, i.e., they cannot transmit and receive simultaneously.
- Anchors are placed randomly on the surface, and have the ability to move within the operating area. The anchors are equipped with GPS and can determine their positions which will be broadcast to the sensor nodes. It is assumed that the probability density function (pdf) of the distance between the anchors is known, $f_D(z)$. It is further assumed that the sensor nodes are located randomly in an operating area according to some probability density function. The sensor nodes can move in the area, but within the localization process, their position is assumed to be constant. The pdf of the distance between a sensor node and an anchor is $g_D(z)$. These pdfs can be estimated from the empirical data gathered during past network operations.
- We consider a single-hop network where all the nodes are within the communication range of each other.
- The received signal strength (which is influenced by path-loss, fading and shadowing) is a function of transmission distance. Consequently, the probability of a packet loss is a function of distance between any pair of nodes in the network.

The considered localization algorithms are assumed to be based on ranging, whereby a sensor node determines its distance to several anchors via ToF or round-trip-time (RTT). Each sensor node can determine its location if it receives at least K different localization packets from K different anchors. The value of K depends on the geometry (2-D or 3-D), and other

factors such as whether depth of the sensor node is available, or whether sound speed estimation is required. The value of K is usually 3 for a 2-D operating environment with known sound speed and 4 for a 3-D one. In a situation where the underwater nodes are equipped with pressure sensors, three different successful packets would be enough for a 3-D localization algorithm [18].

The localization procedure starts either periodically for a predetermined duration (in a synchronized network), or upon receiving a request from a sensor node (in any kind of network, synchronous or asynchronous) as explained below.

Periodic localization: If all the nodes in the network including anchors and sensor nodes are synchronized with each other, a periodic localization approach may be employed. In this approach, after the arrival of a packet from the jth anchor, the mth sensor node estimates its distance to that anchor as $\hat{d}_{m,j} = c(\hat{t}^{\mathrm{R}}_{m,j} - t^{\mathrm{T}}_{j})$ where c is the sound speed, t^{T}_{j} is the time at which the anchor transmits its packet, and $\hat{t}^{\mathrm{R}}_{m,j}$ is the estimated time at which the sensor node receives this packet. The departure time t^{T}_{j} is obtained by decoding the received packet (the anchor inserts this information into the localization packet), and the arrival time $\hat{t}^{\mathrm{R}}_{m,j}$ can be calculated by correlating the received signal with the known training sequence (or similar procedures). The estimated time of arrival is related to the actual arrival time through $\hat{t}^{\mathrm{R}}_{m,j} = t^{\mathrm{R}}_{m,j} + n_{m,j}$, where $n_{m,j}$ is zero-mean Gaussian noise with power $\sigma^2_{m,j}$ which varies with distance and can be modeled as [19]

$$\sigma^2_{m,j} = k_E d^{n_0}_{m,j}, \tag{1}$$

with $d_{m,j}$ the distance between the jth anchor and the sensor node, n_0 the path-loss exponent (spreading factor), and k_E a constant that depends on system parameters (such as signal bandwidth, sampling frequency, channel characteristics, and noise level). In periodic localization, sensor nodes are not required to be synchronized with the anchors. If they are not synchronized, they can calculate the time-differences of arrival (TDoAs) from the measured ToFs; however, we will not consider this situation in our calculation.

On-demand localization: In this procedure (which can be applied to a synchronous or an asynchronous network) a sensor node initiates the localization process. It transmits a high-power frequency tone immediately before the request packet. The tone wakes up the anchors from their idle mode, and puts them into the listening mode. The request packet may also be used for a more accurate estimation of the arrival time. We assume that all the anchors have been correctly notified by this frequency tone. After the anchors have received the wake up tone, they reply with localization packets. The time when the request has been received by an anchor, $t^{\mathrm{R}}_{j,m}$, and the time t^{T}_{j} at which a localization packet is transmitted are included in the localization packet. This information will be used by the sensor node to estimate its round-trip-time (which is proportional to twice the distance) to the anchor. The round-trip-time can be modeled as

$$\hat{t}^{\mathrm{RTT}}_{m,j} = (t^{\mathrm{R}}_{m,j} - t^{\mathrm{T}}_{m}) - (t^{\mathrm{R}}_{j,m} - t^{\mathrm{T}}_{j}) + n_{j,m} + n_{m,j}, \tag{2}$$

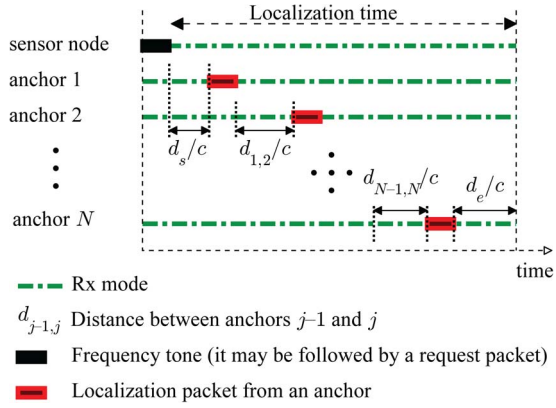

Fig. 1. Packet transmission from anchors in the collision-free scheme. Here, each anchor transmits its packets according to its index value (ID number). All links between anchors are assumed to function properly in this figure (there are no missing links).

where t^{T}_{m} is the transmission time of the request signal from the sensor node. Therefore, the estimated distance to anchor j is

$$\hat{d}_{m,j} = \frac{1}{2} c \hat{t}^{\mathrm{RTT}}_{m,j}. \tag{3}$$

After the sensor node estimates its location, it broadcasts its position to other sensor nodes. This enables the sensor nodes which have overheard the localization process to estimate their positions without initializing another localization task [20].

The time it takes for an underwater node to gather at least K different packets from K different anchors is called the localization time. In the next section, we formally define the localization time, and show how it can be minimized for the collision-free and collision-tolerant packet transmission schemes.

III. Packet Scheduling

A. Collision-Free Packet Scheduling

Collision-free localization packet transmission is analyzed in [16], where it is shown that in a fully-connected (single-hop) network, based on a given sequence of the anchors' indices, each anchor has to transmit immediately after receiving the previous anchor's packet. Furthermore, it is shown that there exists an optimal ordering sequence which minimizes the localization time. However, to obtain that sequence, a fusion center is required to know the positions of all the anchors. In a situation where this information is not available, we may assume that anchors simply transmit in order of their ID numbers as illustrated in Fig. 1.

In the event of a packet loss, a subsequent anchor will not know when to transmit. If an anchor does not receive a packet from a previous anchor, it waits for a predefined time (counting from the starting time of the localization process), and then transmits its packet, similarly as introduced in [21]. With a slight modification of the result from [21], the waiting time for the jth anchor who has not received a packet from its previous anchor, could be as short as $t_k + (j-k)(T_p + \frac{D_{\mathrm{aa}}}{c})$, where k is the index of the anchor whose packet is the last one which has been received by the jth anchor, t_k is the time at which this packet

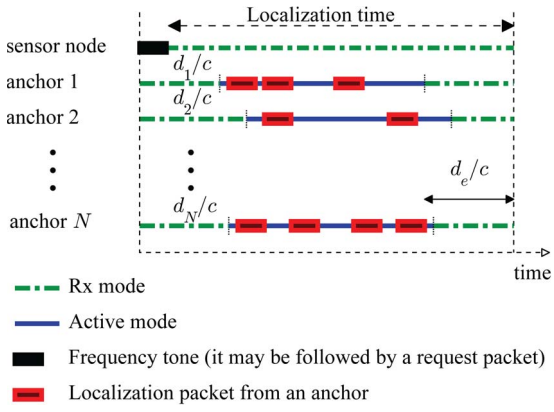

Fig. 2. Packet transmission from anchors in the collision-tolerant scheme. Here, each anchor transmits its packets at random according to a Poisson distribution.

TABLE I
POSSIBLE TIMES THAT ANCHOR j TRANSMITS ITS PACKET

	t_j	with probability
1	$t_{j-1}+\frac{d_{j,j-1}}{c}+T_{\rm p}$	$1-p_l(d_{j,j-1})$
2	$t_{j-2}+2\left(\frac{D_{\rm aa}}{c}+T_{\rm p}\right)$	$[1-p_l(d_{j,j-2})]p_l(d_{j,j-1})$
$\vdots$	$\vdots$	$\vdots$
$j-k$	$t_k+(j-k)\left(\frac{D_{\rm aa}}{c}+T_{\rm p}\right)$	$[1-p_l(d_{j,k})]\Pi_{m=k+1}^{j-1}p_l(d_{j,m})$
$\vdots$	$\vdots$	$\vdots$
$j-1$	$\frac{D_{\rm r}}{c}+(j-1)\left(\frac{D_{\rm aa}}{c}+T_{\rm p}\right)$	$\Pi_{m=1}^{j-1}p_l(d_{j,m})$

was transmitted from the kth anchor (counting from the starting time of the localization process), c is the sound speed, $\frac{D_{\rm aa}}{c}$ is the maximum propagation delay between two anchors, and T_p is the packet length. The packet length is related to the system bandwidth B (or symbol time $T_s \approx \frac{1}{B}$), number of bits in each symbol b_s, number of bits in each packet b_p, and guard time T_g as formulated in

$$T_p = T_g + \frac{b_p}{b_s}T_s. \tag{4}$$

Under this condition, the transmission time of the jth anchor t_j can be selected from one of the values listed in Table I where $D_{\rm r} = D_{\rm sa}$ in on-demand localization which is the distance corresponding to the maximally separated sensor-anchor pair, and $D_{\rm r} = 0$ in periodic localization, $t_1 = 0$ for periodic localization, and $t_1 = \frac{d_{\rm s}}{c}$ for on-demand localization, with $d_{\rm s}$ the distance between the first anchor and the sensor who sent the request packet, and $p_l(d_{i,j})$ is the probability of packet loss between two anchors located $d_{i,j}$ meters away from each other. The packet loss can be defined as

$$p_l(d) = \int_{\gamma_0 N_0 B}^{\infty} f_{X_0|d}(x)dx \tag{5}$$

where N_0B is the noise power, γ_0 is the minimum SNR at which a received packet can be detected at the receiver, and given the distance between two nodes, d, $f_{X_0|d}(x)$ is the conditional pdf of the received signal power which will be derived in the next subsection. The first row of Table I indicates that no packet loss (with probability $1-p_l(d_{j,j-1})$) occurs between the jth and $(j-1)$th anchor, and the jth anchor transmits after it receives the packet from the $(j-1)$th anchor. The second row denotes that there is a packet loss between the jth and $(j-1)$th anchor (with probability $p_l(d_{j,j-1})$), but there is no packet-loss between the jth and $(j-2)$th anchor (with probability $1-p_l(d_{j,j-2})$). Therefore, according to the protocol, the jth anchor waits until $t_{j-2}+2(\frac{D_{\rm aa}}{c}+T_{\rm p})$ before it transmits its packet. The last row of Table I specifies that the jth anchor has lost all the packets from all anchors, and as a result transmits at a worst possible time to avoid any collision.

Since $d_{i,j}$ for $j=1,\ldots,N-1$, and $d_{\rm s}$ are independent of each other, the average time at which the jth anchor transmits its packet can be obtained as

$$\begin{aligned}\bar{t}_j =& (1-\bar{p}_l)\sum_{k=1}^{j-1}\bar{t}_k\bar{p}_l^{j-k-1} + T_{\rm p}(1-\bar{p}_l) + \frac{\bar{d}}{c} - \frac{\bar{dp}_l}{c}\\ &+(1-\bar{p}_l)\left(\frac{D_{\rm aa}}{c}+T_{\rm p}\right)\sum_{k=2}^{j-1}k\bar{p}_l^{k-1}\\ &+(j-1)\left(\frac{D_{\rm aa}}{c}+T_{\rm p}\right)\bar{p}_l^{j-1} + \frac{D_{\rm r}}{c}\bar{p}_l^{j-1}\end{aligned} \tag{6}$$

where $\bar{p}_l$, $\bar{d}$, and $\bar{dp}_l$ are the expected values of $p_l(d_{i,j})$, $d_{i,j}$, and $d_{i,j}p_l(d_{i,j})$, respectively.

The average localization time of a collision-free scheme can be obtained as

$$T_{\rm CF}^{\rm avg} = \bar{t}_N + T_p + \frac{D_{\rm sa}}{c}, \tag{7}$$

where $\frac{D_{\rm sa}}{c}$ is added to ensure that the last transmitted packet from the Nth anchor reaches the furthest point in the operating area.

In the best case there is no packet loss between the anchors and the average localization time reaches its minimum value at

$$T_{\rm CF}^{\rm low} = (N-1)\frac{\bar{d}}{c} + \frac{\bar{d}_s}{c} + NT_p + \frac{D_{\rm sa}}{c}, \tag{8}$$

where $\bar{d}_s$ is the average distance between a sensor node and an anchor. In the worst case, all the packets between the anchors are lost, and the requesting sensor node is the farthest from the initiating anchor. This case yields the longest localization time given by

$$T_{\rm CF}^{\rm upp} = NT_p + (N-1)\frac{D_{\rm aa}}{c} + \frac{D_{\rm sa}}{c} + \frac{D_{\rm sa}}{c}, \tag{9}$$

which is equivalent to a packet transmission based on time division multiple access (TDMA) with time-slot duration $T_p + \frac{D}{c}$ (assuming $D = D_{\rm sa} = D_{\rm aa}$).

Another figure of merit is the probability with which a node can localize itself. If this probability is required to be above a design value P_{ss}, the necessary number of anchors which also minimizes $T_{\rm CF}^{\rm avg}$ ($T_{\rm CF}^{\rm avg}$ is an increasing function of N) is determined as the smallest N for which

$$P_{\rm CF}^{\rm loc} = \sum_{k=K}^{N}\binom{N}{k}p_{\rm CF}^k(1-p_{\rm CF})^{N-k} \geq P_{ss} \tag{10}$$

where p_{CF} is the probability that a transmitted packet reaches a sensor node correctly, and it can be calculated as

$$p_{\mathrm{CF}} = \int_{\gamma_0 N_0 B}^{\infty} f_{X_0}(x)dx, \tag{11}$$

where $f_{X_0}(x)$ is the pdf of the received signal power.

B. Collision-Tolerant Packet Scheduling

To avoid the need for coordination among anchor nodes, in a collision-tolerant packet scheduling, anchors work independently of each other. During a localization period or upon receiving a request from a sensor node, they transmit randomly, e.g., according to a Poisson distribution with an average transmission rate of λ packets per second. Packets transmitted from different anchors may now collide at a sensor node, and the question arises as to what is the probability of successful reception. This problem is a mirror image of the one investigated in [22] where sensor nodes transmit their packets to a common fusion center. Unlike [22] however, where the sensors know their location, and power control fully compensates for the known path-loss, path-loss is not known in the present scenario, and there is no power control. The average received signal strength is thus different for different links (this signal strength, along with a given fading model, determines the probability of packet loss). In this regard, the signal received at the mth sensor node from the jth anchor is

$$v_{m,j}(t) = c_{m,j}v_j(t) + i_m(t) + w_m(t), \tag{12}$$

where $v_j(t)$ is the signal transmitted from the jth anchor, $c_{m,j}$ is the channel gain, $w_m(t)$ is the additive white Gaussian noise with power N_0B, and $i_m(t)$ is the interference caused by other anchors whose packets overlap with the desired packet,

$$i_m(t) = \sum_{k\neq j} c_{m,k}v_k(t-\tau_k), \tag{13}$$

with τ_k being the difference in the arrival times of the interfering signals w.r.t. the desired signal which is modeled as an exponentially distributed random variable. The signal-to interference-plus-noise-ratio (SINR) at the receiver depends on the interference level, and is given by

$$\gamma = \frac{X_0}{I_0 + N_0 B}, \tag{14}$$

where $X_0 = |c_{m,j}|^2 P_0$ is the power of the signal of interest with P_0 the anchor's transmit power, and where I_0 is the total interference power which can be expressed as

$$I_0 = \sum_{i=1}^{q} |c_{m,k_i}|^2 P_0 \tag{15}$$

with q the number of interferers, and k_i the index of the ith interferer. We can express the signal power as

$$|c_{m,j}|^2 = a_{\mathrm{PL}}^{-1}(d_{m,j})e^{g_{m,j}}|h_{m,j}|^2, \tag{16}$$

where $g_{m,j} \sim \mathcal{N}(0,\sigma_g^2)$ models the large scale log-normal shadowing, $h_{m,j} \sim C\mathcal{N}(\bar{h},\sigma_h^2)$ models the small scale fading, and a_{PL} models the path-loss attenuation which can be formulated as [23]

$$a_{\mathrm{PL}}(d_{i,j}) = \alpha_0 \left(\frac{d_{i,j}}{d_0}\right)^{n_0} a(f)^{d_{i,j}} \tag{17}$$

where α_0 is a constant, d_0 is the reference distance, n_0 is the path-loss exponent, and $a(f)$ is the frequency-dependent absorption coefficient. For localization, where the bandwidth is not large, $\alpha(f)$ can be approximated by a constant.

The pdf of the received signal power, $f_{X_0}(x)$ can be obtained numerically. Since a_{PL}, $g_{m,j}$ and $h_{m,j}$ are independent random variables, we calculate the pdfs of $10\log|h_{m,j}|^2$, $10\log e^{g_{m,j}}$, and $-10\log a_{\mathrm{PL}}$ separately. Then we convolve them which results in $f_{X_0,dB}(x_{dB})$. With a simple change of variables $x = 10^{0.1x_{dB}}$ we can find $f_{X_0}(x)$, and the pdf of the interference can be obtained as

$$f_{I_0}(x) = \underbrace{f_{X_0}(x) * f_{X_0}(x) * \ldots * f_{X_0}(x)}_{q\,\text{times}}. \tag{18}$$

The probability that a packet is received correctly by a sensor node is then [22]

$$p_s = \sum_{q=0}^{N-1} P(q)p_{s|q}, \tag{19}$$

where $P(q) = \frac{(2N\lambda T_p)^q}{q!}e^{-2N\lambda T p}$ is the probability that q packets interfere with the desired packet, and $p_{s|q}$ is the probability that the desired packet "survives" under this condition,

$$p_{s|q} = \begin{cases} \int_{\gamma_0 N_0 B}^{\infty} f_{X_0}(x)dx & q = 0 \\ \int_{\gamma_0}^{\infty}\int_{N_0 B}^{\infty} f_{X_0}(\gamma w) f_{I_0}(w - N_0 B) w dw d\gamma & q \geq 1 \end{cases} \tag{20}$$

where $w = I_0 + N_0 B$.

In addition, it should be noted that multiple receptions of a packet from an anchor does not affect the probability of self-localization (localization coverage), but in case where a sensor node is able to localize itself, multiple receptions of a packet from an anchor affects the accuracy of the localization (see Section IV).

If we assume that the packets transmitted from the same anchor fade independently, the probability of receiving a useful packet from an anchor during the transmission time T_{T} can now be approximated by [22]

$$p_{\mathrm{CT}} = 1 - e^{-p_s\lambda T_{\mathrm{T}}}, \tag{21}$$

and the probability that a sensor node accomplishes self-localization using N anchors can be obtained as

$$P_{\mathrm{CT}}^{\mathrm{loc}} = \sum_{k=K}^{N} \binom{N}{k} p_{\mathrm{CT}}^k (1 - p_{\mathrm{CT}})^{N-k}, \tag{22}$$

which is equivalent to the probability that a node receives at least K different localization packets.

It can be shown that $P_{\mathrm{CT}}^{\mathrm{loc}}$ is an increasing function of T_{T} (see Appendix A), and as a result for any value of $p_s\lambda \neq 0$, there is a T_{T} that leads to a probability of self-localization equal to or greater than P_{ss}. The minimum value for the required T_{T} can

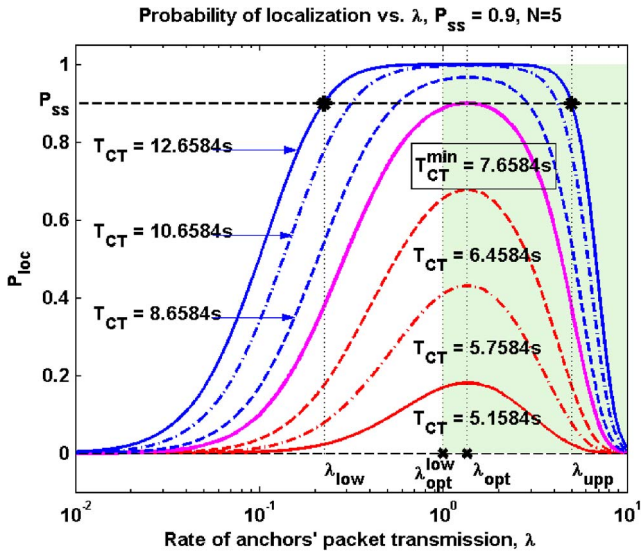

Fig. 3. Probability of successful localization for different values of λ and T_{CT}.

be obtained at a point where $p_s\lambda$ is maximum (λ_{opt}). It can be proven that the lower bound of λ_{opt} is $\lambda_{\mathrm{opt}}^{\mathrm{low}} = \frac{1}{2NT_p}$, and its upper bound is $\frac{N+1}{2NT_p}$ (see Appendix B). These points will be illustrated via numerical examples in Section VI (cf. Fig. 3).

Given the number of anchors N, and a desired probability of successful self-localization P_{ss}, one can determine p_{CT} from (22), while λ and the minimum localization time can be determined jointly from (19) and (21). Similarly as in the collision-free scheme, we then add the time of request $\frac{d_s}{c}$, and the maximum propagation delay between a sensor-anchor pair $\frac{D_{\mathrm{sa}}}{c}$ to the (minimum) T_{T} that is obtained from (19) and (21). The so-obtained value represents the (minimum) localization time ($T_{\mathrm{CT}}^{\mathrm{min}}$) T_{CT}, for the collision-tolerant scheme.

IV. Self-Localization Process

We have seen that a sensor node requires at least K distinct packets (or time-of-flight measurements) to determine its location. However, it may receive more than K different packets, as well as some replicas, i.e., q_j packets from anchor j, where $j = 1,\ldots,N$. In this case, a sensor uses all of this information for self-localization. Note that in the collision-free scheme, q_j is either zero or one; however, in the collision-tolerant scheme q_j can be more than 1. Packets received from the jth anchor can be used to estimate the sensor node's distance to that anchor, and the redundant packets add diversity (or reduce measurement noise) for this estimate. In the next two subsections, we show how all of the correctly received packets can be used in a localization algorithm, and how the CRB of the location estimate can be obtained for the proposed scheduling schemes.

A. Localization Algorithm

After the anchors transmit their localization packets, each sensor node has Q measurements. Each measurement is contaminated by noise whose power is related to the distance between the sensor and the anchor from which the measurement has been obtained. The lth measurement obtained from the jth anchor is related to the sensor's position $\mathbf{x}$ (sensor index is omitted for simplicity) as

$$\hat{t}_l = f(\mathbf{x}) + n_l, \tag{23}$$

where n_l is the measurement noise (see (1)) and $f(\mathbf{x})$ is

$$f(\mathbf{x}) = \frac{1}{c}\|\mathbf{x} - \mathbf{x}_j\|_2 \tag{24}$$

where $\mathbf{x}_j$ is the jth anchor's position. Stacking all the measurements gives us a $Q \times 1$ vector $\hat{\mathbf{t}}$. The number of measurements is given by

$$Q = \sum_{j=1}^{N} q_j, \tag{25}$$

where q_j is the number of measurements which are obtained correctly from the jth anchor. In CFS, q_j is a Bernoulli random variable with success probability $P_j^1 = P(q_j = 1) = 1 - p_l(d_j)$ where d_j is the distance between the sensor node and the jth anchor. In CTS q_j is a Poisson random variable with distribution

$$P_j^n = P(q_j = n) = \frac{(p_s\lambda T_{\mathrm{T}})^n}{n!} e^{-\lambda T_{\mathrm{T}} p_{s|\mathbf{d}}^j}, \tag{26}$$

where $p_{s|\mathbf{d}}^j$ is the conditional probability that a sensor node correctly receives a packet from the jth anchor, knowing its distance from all anchors (elements of $\mathbf{d}$). This pdf can be found from the conditional pdf of the received signal and the interference power (see (19) and (20)).

Since the measurement errors are independent of each other, the maximum likelihood solution for $\mathbf{x}$ is given by

$$\hat{\mathbf{x}} = \arg\min_{\mathbf{x}} \left\|\hat{\mathbf{t}} - \mathbf{f}(\mathbf{x})\right\|_2, \tag{27}$$

which can be calculated using a method such as the Gauss-Newton algorithm specified in Algorithm 1. In this algorithm, η controls the convergence speed, $\nabla\mathbf{f}(\mathbf{x}^{(i)}) = [\frac{\partial f_1}{\partial \mathbf{x}}, \frac{\partial f_2}{\partial \mathbf{x}}, \ldots, \frac{\partial f_Q}{\partial \mathbf{x}}]^T_{\mathbf{x}=\mathbf{x}^{(i)}}$ represents the gradient of the vector $\mathbf{f}$ w.r.t. the variable $\mathbf{x}$ at $\mathbf{x}^{(i)}$, $\mathbf{x}^{(i)}$ is the estimate in the ith iteration, and $\frac{\partial f_l}{\partial \mathbf{x}} = [\frac{\partial f_l}{\partial x}, \frac{\partial f_l}{\partial y}, \frac{\partial f_l}{\partial z}]^T$ where $l = 1,\ldots,Q$. Here, I and ε are the user-defined limits on the stopping criterion. The initial guess is also an important factor and can be determined through triangulation, similarly as explained in [24].

Algorithm 1 Gauss-Newton Algorithm

Start with an initial location guess.
Set $i = 1$ and $E = \infty$.
while $i \le I$ and $E \ge \varepsilon$ **do**
  Next state:
    $\mathbf{x}^{(i+1)} = \mathbf{x}^{(i)} -$
    $\eta(\nabla\mathbf{f}(\mathbf{x}^{(i)})^T\nabla\mathbf{f}(\mathbf{x}^{(i)}))^{-1}\nabla\mathbf{f}(\mathbf{x}^{(i)})^T(\mathbf{f}(\mathbf{x}^{(i)}) - \hat{\mathbf{t}})$
    $E = \|\mathbf{x}^{(i+1)} - \mathbf{x}^{(i)}\|$
    $i = i + 1$
end while
$\hat{\mathbf{x}} = \mathbf{x}^{(i)}$

B. Cramér-Rao Bound

The Cramér-Rao bound is a lower bound on the variance of any unbiased estimator of a deterministic parameter. In this subsection, we derive the CRB for the location estimate of a sensor node.

To find the CRB, the Fisher information matrix (FIM) has to be calculated. The Fisher information is a measure of information that an observable random variable $\hat{\mathbf{t}}$ carries about an unknown parameter $\mathbf{x}$ upon which the pdf of $\hat{\mathbf{t}}$ depends. The elements of the FIM are defined as

$$\mathbf{I}(\mathbf{x})_{i,j} = -\mathbb{E}\left[\frac{\partial^2 \log h(\hat{\mathbf{t}};\mathbf{x})|\mathbf{x}}{\partial x_i \partial x_j}\right] \tag{28}$$

where $\mathbf{x}$ is the location of the sensor node, $h(\hat{\mathbf{t}};\mathbf{x})$ is the pdf of the measurements parametrized by the value of $\mathbf{x}$, and the expected value is over the cases where the sensor is localizable.

In a situation where the measurements (ToFs or RTTs between a sensor node and the anchors) are contaminated with Gaussian noise (whose power is related to the mutual distance between a sensor-anchor pair), the elements of the FIM can be formulated as

$$\mathbf{I}(\mathbf{x})_{i,j} = \frac{1}{P^{\text{loc}}} \sum_{\substack{q_N=0}}^{Q_N} \cdots \sum_{q_2=0}^{Q_2} \sum_{q_1=0}^{Q_1} \underset{\text{s.t.}\{q_1,\ldots,q_N\} \text{ enable self-localization}}{} \times \left\{ \frac{\partial \mathbf{f}}{\partial x_i}^T \mathbf{R}_w^{-1} \frac{\partial \mathbf{f}}{\partial x_j} + \frac{1}{2}\text{tr}\left[\mathbf{R}_w^{-1}\frac{\partial \mathbf{R}_w}{\partial x_i}\mathbf{R}_w^{-1}\frac{\partial \mathbf{R}_w}{\partial x_j}\right]\right\} \Pi_{j=1}^{N} P_j^{q_j} \tag{29}$$

where P^{loc} is the localization probability (see (10) and (22)), $Q_i = 1$ for CFS, and ∞ for CTS, $\mathbf{R}_w$ is the $Q \times Q$ noise covariance matrix

$$\frac{\partial \mathbf{R}_w}{\partial x_i} = \text{diag}\left(\frac{\partial [\mathbf{R}_w]_{11}}{\partial x_i}, \frac{\partial [\mathbf{R}_w]_{22}}{\partial x_i}, \ldots, \frac{\partial [\mathbf{R}_w]_{QQ}}{\partial x_i}\right), \tag{30}$$

and

$$\frac{\partial \mathbf{f}}{\partial x_i} = \left[\frac{\partial f_1}{\partial x_i}, \frac{\partial f_2}{\partial x_i}, \ldots, \frac{\partial f_Q}{\partial x_i}\right]^T, \tag{31}$$

with f_i a ToF or RTT measurement.

Once the FIM has been computed, the lower bound on the variance of the estimation error can be expressed as $\text{CRB} = \sum_{i=1}^{3} \text{CRB}_{x_i}$ where CRB_{x_i} is the variance of the estimation error in the ith variable, defined as

$$\text{CRB}_{x_i} = \left[I^{-1}(\mathbf{x})\right]_{ii}. \tag{32}$$

Note that the CRB is meaningful if a node is localizable ($\frac{1}{P^{\text{loc}}}$ in (29)), meaning that a sensor node has at least K different measurements. Hence, only $\sum_{k=K}^{N}\binom{N}{k}$ possible states have to be considered to calculate (29) for collision-free scheduling, while the number of states is countless for collision-tolerant scheduling. Nonetheless, it can be shown that the number of possible states in CTS can be dropped to that of CFS (see Appendix C).

TABLE II
VALUES OF θ_s AND θ_e BASED ON DISTANCE d

distance	θ_s	θ_e
$0 \le d \le D_y$	0	$\frac{\pi}{2}$
$D_y \le d \le D_x$	0	$\sin^{-1}\frac{D_y}{d}$
$D_y \le d \le \sqrt{D_x^2 + D_y^2}$	$\cos^{-1}\frac{D_x}{d}$	$\sin^{-1}\frac{D_y}{d}$

V. Energy Consumption

In this section, we investigate the average energy consumed by all the anchors during the localization. In CFS, the receiver of anchor j is on for t_j seconds, and its transmitter is on only for T_p seconds. With power consumption P_{L} in listening mode and P_{T} in transmitting mode, the average energy consumption in CFS is

$$E_{\text{CF}}^{\text{avg}} = NT_pP_{\text{T}} + \sum_{j=1}^{N} \bar{t}_j P_{\text{L}}, \tag{33}$$

where the energy consumed for processing is ignored. As is clear from (6), an anchor with a higher index value has to listen to the channel longer, and consequently consumes more energy in comparison with the one that has a lower index. To overcome this problem, anchors can swap indices between localization procedures.

In CTS, the anchors do not need to listen to the channel and they only transmit at an average rate of λ packets per second. The average energy consumption is thus

$$E_{\text{CT}}^{\text{avg}} = \lambda T_{\text{T}} N T_p P_{\text{T}}. \tag{34}$$

For ($\frac{P_{\text{L}}}{P_{\text{T}}} < \frac{NT_{\text{p}}(\lambda T_{\text{T}}-1)}{\sum_{j=1}^{N}\bar{t}_j}$), the average energy consumption of CTS is always greater than that of CFS. However, as λ gets smaller (or equivalently T_{CT} gets larger), the energy consumption of CTS reduces.

VI. Numerical Results

To illustrate the results, a 2-D rectangular-shape operating area with length D_x and width D_y is considered with uniformly distributed anchors and sensors. There is no difference in how the anchors and sensor nodes are distributed, and therefore we have $f_D(d) = g_D(d)$ which can be obtained as [26]

$$f_D(d) = \frac{2d}{D_x^2 D_y^2}\left[d^2(\sin^2\theta_e - \sin^2\theta_s) + 2D_xD_y(\theta_e - \theta_s) + 2D_xd(\cos\theta_e - \cos\theta_s) - 2D_yd(\sin\theta_e - \sin\theta_s)\right] \tag{35}$$

where θ_s and θ_e are related to d as given in Table II.

The parameter values for the numerical results are listed in Table III, and used for all examples.

The number of bits in each packet is set to $b_p = 200$ which is sufficient for the position information of each anchor, time of transmission, (arrival time of the request packet), and the training sequence. Assuming QPSK modulation ($b_s = 2$), guard time $T_g = 50$ ms, and a bandwidth of $B = 2$ kHz the localization packet length is $T_p = 100$ ms (see (4)). In addition, k_E is set

TABLE III
SIMULATION PARAMETERS. NOTE THAT, IN THIS TABLE SOME PARAMETERS SUCH AS N, D_{aa}, T_g, etc. ARE RELATED TO OTHER PARAMETERS, e.g., N DEPENDS ON THE VALUES OF THE $\bar{p}_l$, AND P_{ss}

Description	Para.	Value	Unit
Number of anchor nodes	N	5	-
Number of sensor nodes	M	100	-
Sound speed	c	1500	m/s
Number of required different packets	K	3	-
Area size in x-axis	D_x	$3c$	m
Area size in y-axis	D_y	$3c$	m
Maximum anchor-anchor distance	D_{aa}	$3c\sqrt{2}$	m
Maximum anchor-sensor distance	D_{sa}	$3c\sqrt{2}$	m
Guard time for localization packet	T_g	50	ms
Number of bits per sample	b_s	2	-
Number of bits per packet	b_p	200	-
System bandwidth	B	2	kHz
Localization packet length	T_p	100	ms
Noise power	N_0B	100	dB re 1μPa
ToF noise power coefficient	k_E	10^{-10}	
Transmit power	P_0	166	dB re 1μPa
Reference distance	d_0	1	m
Power coefficient	α_0	1	m
Path-loss exponent	n_0	1.4	-
Fading variance	$\bar{h}$	$\sqrt{1/4}$	-
Shadowing variance	σ_h	$\sqrt{3/4}$	-
Fading mean	σ_g	0	dB
Absorption coefficient	$a(f)$	1	dB/km
Required SNR for packet detection	γ_0	6	dB
Request packet arrival delay	d_s/c	0	s
Required probability of successful localization	P_{ss}	0.99	-

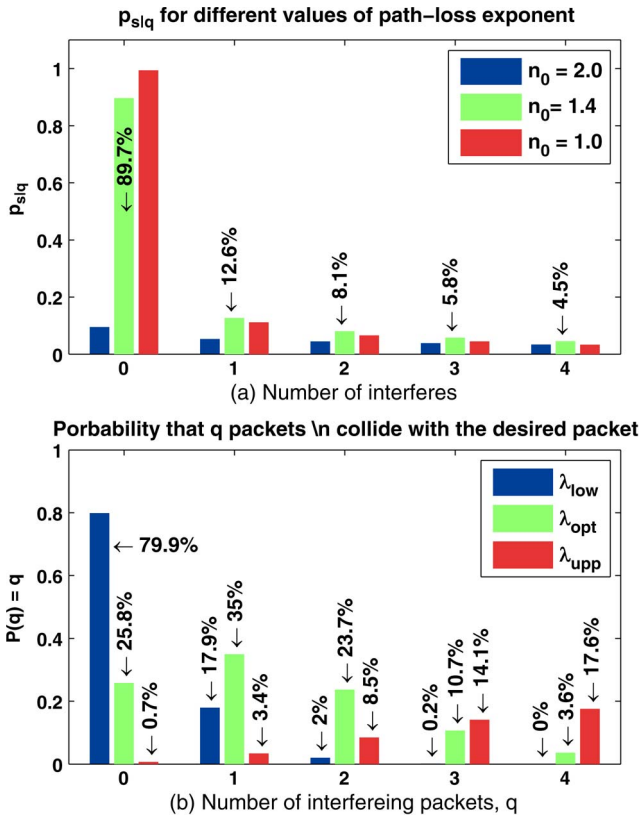

Fig. 4. (a) Probability of successful packet reception versus different number of interferers. (b) Probability that q interferers collide with the desired packet. For this figure, λ_{low}, λ_{opt} and λ_{upp} are chosen from Fig. 3.

to 10^{-10} which is approximately equivalent to 1.9 m range accuracy at 1 km away from an anchor. Moreover, to keep the transmitted packets from an anchor in CTS independent of each other, we set $\sigma_g = 0$ (no shadowing effect) for the simulations. Fig. 3 shows the probability of successful self-localization in the collision-tolerant scheme as a function of λ and the indicated value for T_{CT}. It can be observed that there is an optimal value of λ (denoted by λ_{opt}) which corresponds to the minimal value of T_{CT} ($T_{\text{CT}}^{\min}$) which satisfies $P_{\text{CT}}^{\text{loc}} \geq P_{ss}$. The highlighted area in Fig. 3 shows the predicted region of λ_{opt} (obtained in Appendix B). As it can be seen, λ_{opt} is close to $\lambda_{\text{opt}}^{\text{low}}$, and it gets closer to this value as $P_{s|q>0}$ gets smaller. In addition, for the values of T_{CT} greater than $T_{\text{CT}}^{\min}$, a range of values for $\lambda \in [\lambda_{\text{low}}, \lambda_{\text{upp}}]$ can attain the desired probability of self-localization. In this case, the lowest value for λ should be selected to minimize the energy consumption.

Fig. 4 shows the probability of correct packet reception versus the number of interferers (the desired P_{ss} is set to 0.90 in this example) for different values of the path-loss exponent n_0. When there is no interference, the probability of packet reception is high. Yet, when there is an interferer, the chance of correct reception of a packet becomes small (0.126 for $n_0 = 1.4$), and as the number of interferers grows, it gets smaller.

The probability that two or more packets overlap is also depicted in part (b) of this figure for the three values of λ shown in Fig. 3. It can be seen that as the value of λ is reduced from λ_{opt} (which is equivalent to a larger T_{CT}), the probability of collision becomes smaller. The chance of correct packet reception thus increases, and the energy consumption reduces as explained in Section V. In addition, it can be observed that although using λ_{upp} results in the same performance as λ_{low}, it relies on the packets that have survived collisions, which is not energy-efficient in practical situations neither for anchors (required energy for multiple packet transmissions) nor for sensor nodes (processing energy needed for packet detection).

Part (a) of Fig. 5 shows the time required for localization versus the transmit power. As P_0 increases, $\bar{p}_l$ gets smaller, and consequently fewer anchors are required for collision-free localization. In Fig. 5, for a given P_0, the number of anchors N is calculated using (10), which is then used to calculate the minimum required time for the collision-free and collision-tolerant localization. Each fall in $T_{\text{CF}}^{\text{upp}}$ in CFS indicates that the number of anchors has been decreased by one. We also note that for a given number of anchors, the upper and lower bounds of T_{CF} are constant over a range of P_0 values; however, the actual performance of both schemes becomes better as P_0 grows. The collision-tolerant approach performs better for a wide range of P_0 values, and as the number of anchors decreases, its performance slightly degrades. In part (b) of Fig. 5, we calculate the ratio $\frac{P_{\text{L}}}{P_{\text{T}}}$ below which the average energy of CTS is greater than that of CFS. The ratio of $E_{\text{CF}}^{\text{avg}}/E_{\text{CT}}^{\text{avg}}$ is a linear function of $\frac{P_{\text{L}}}{P_{\text{T}}}$, and as P_0 increases for larger values of $\frac{P_{\text{L}}}{P_{\text{T}}}$, the average energy consumption of CTS becomes greater than that of CFS. In practice, for a range of 6 km the $\frac{P_{\text{L}}}{P_{\text{T}}}$ is less than $\frac{1}{100}$ [25], and this means that CTS consumes more energy.

Many factors such as noise power or packet length are directly dependent on the operating frequency and the system bandwidth. Assuming single-hop communication among the sensor nodes, an optimum frequency band exists for a given

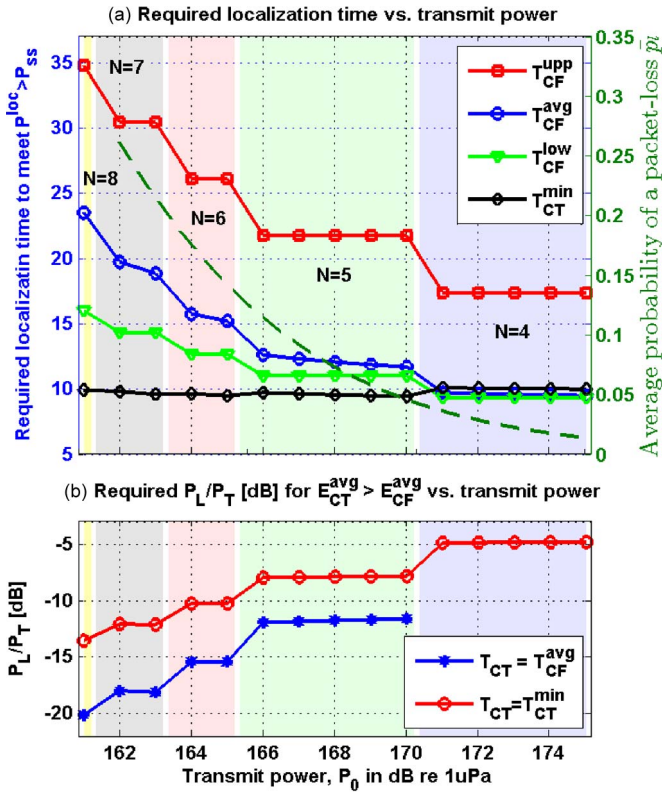

Fig. 5. (a) Effect of transmit power on the minimum time required for localization, and the average probability of a packet-loss $\bar{p}_l$ (dashed-line). (b) The minimum value of $\frac{P_L}{P_T}$ in dB below which the average energy consumption of CTS is greater than that of CFS.

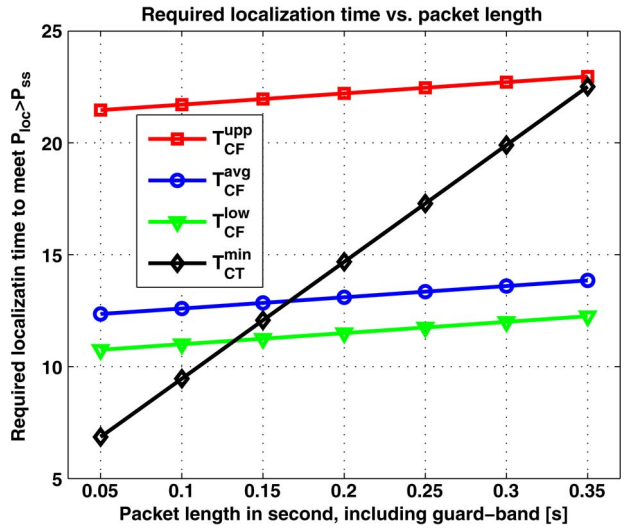

Fig. 6. Effect of packet length on the minimum time required for localization.

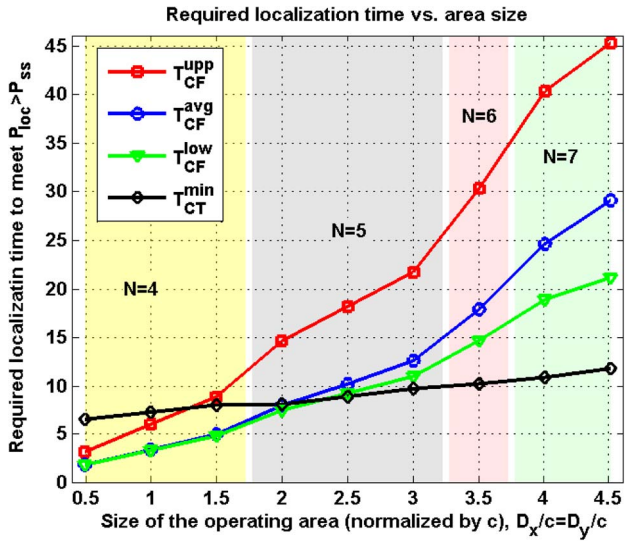

Fig. 7. Effect of the operating area size on the time required localization.

operating area. As the size of the operating area increases, a lower operating frequency (with less bandwidth) is used to compensate for the increased attenuation. Furthermore, as the distance increases, the amount of available bandwidth for the optimum operating frequency also gets smaller [23]. As it was mentioned before, the localization packet is usually short in terms of the number of bits, but its duration (in seconds) still depends on the system bandwidth. Below, we investigate the effect of packet length (or equivalently system bandwidth) on the localization time.

As it is shown in Fig. 6, the length of the localization packet plays a significant role in the collision-tolerant algorithm. The minimum localization time grows almost linearly with T_p in all cases; however, the rate of growth is much higher for the collision-tolerant system than for the collision-free one. At the same time, as shown in Fig. 7, the size of the operating area has a major influence on the performance of the CFS, while that of the CTS does not change very much. It can be deduced that in a network where the ratio of packet length to the maximum propagation delay is low, the collision-tolerant algorithm outperforms the collision-free one in terms of localization time.

The localization accuracy is related to the noise level at which a ToF measurement is taken, and to the anchors' constellation. If a sensor node in a 2-D operating system receives packets from the anchors which are (approximately) located on a line, the sensor node is unable to localize itself (or it experiences a large error). To evaluate the localization accuracy of each algorithm, we considered $M = 100$ sensor nodes, and run a Monte Carlo simulation (10^3 runs) to extract the results. The number of iterations in Algorithm 1 is set to $I = 50$, and the convergence rate is $\eta = \frac{1}{5}$. The T_{CF} was set equal to the average localization time of CFS. In this special case where $T_{\text{CT}}^{\min}$ is lower than $T_{\text{CF}}^{\text{avg}}$, the successful localization probability (P^{loc}) of CTS is greater than that of CFS. The probability distribution of the localization error $\|\hat{\mathbf{x}} - \mathbf{x}\|$ is illustrated in Fig. 8 for both schemes. In this figure, the root mean square error (RMSE), and root CRB (R-CRB) are also shown with the dashed and dash-dotted lines, respectively. It can be observed that in CTS the pdf is concentrated at lower values of the localization error compared to CFS, because each sensor in CTS has a chance of receiving multiple copies of the same packet, and thus reducing the range estimation error.

VII. Conclusion

We have considered two classes of packet scheduling for self-localization in an underwater acoustic sensor network,

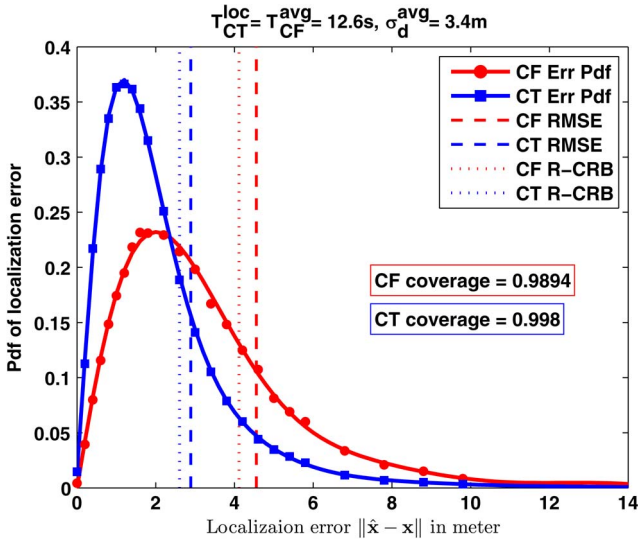

Fig. 8. Probability distribution of the localization error, and its corresponding CRB for CTS and CFS.

one based on a collision-free design and another based on a collision-tolerant design. In collision-free packet scheduling, the time of the packet transmission from each anchor is set in such a way that none of the sensor nodes experiences a collision. In contrast, collision-tolerant algorithms are designed so as to control the probability of collision to ensure successful localization with a pre-specified reliability. We have also proposed a simple Gauss-Newton based localization algorithm for these schemes, and derived their Cramér-Rao lower bounds. The performance of the two classes of algorithms in terms of the time required for localization was shown to be dependent on the circumstances. When the ratio of the packet length to the maximum propagation delay is low, as it is the case with localization, and the average probability of packet-loss is not close to zero, the collision-tolerant protocol requires less time for localization in comparison with the collision-free one for the same probability of successful localization.Except for the average energy consumed by the anchors, the collision-tolerant scheme has multiple advantages. The major one is its simplicity of implementation due to the fact that anchors work independently of each other, and as a result the scheme is spatially scalable, with no need for a fusion center. Furthermore, its localization accuracy is always better than that of the collision-free scheme due to multiple receptions of desired packets from anchors. These features make the collision-tolerant localization scheme appealing from a practical implementation view point. In the future, we will extend our work to a multi-hop network where the communication range of the acoustic modems is much shorter than the size of the operating area.

Appendix A
$P^{\text{loc}}_{\text{CT}}$ Is an Increasing Function of T_{CT}

In this appendix, we show that the probability of successful localization is an increasing function of the localization time. According to (21), and the fact that $p_s\lambda$ is independent of T_{T}, it is clear that p_{CT} is an increasing function of T_{T}. Therefore, $P^{\text{loc}}_{\text{CT}}$ is an increasing function of T_{T} if $P^{\text{loc}}_{\text{CT}}$ is an increasing function of p_{CT}. The derivative of $P^{\text{loc}}_{\text{CT}}$ w.r.t. p_{CT} is

$$\frac{\partial P^{\text{loc}}_{\text{CT}}}{\partial p_{\text{CT}}} = \sum_{k=K}^{N} \binom{N}{k} (k - N p_{\text{CT}}) p_{\text{CT}}^{k-1} (1-p_{\text{CT}})^{N-k-1}. \tag{36}$$

With a simple modification we have

$$\begin{aligned}\frac{\partial P^{\text{loc}}_{\text{CT}}}{\partial p_{\text{CT}}} = {} & \frac{1}{p_{\text{CT}}(1-p_{\text{CT}})} \\ & \times \left\{ \left[\sum_{k=0}^{N} \binom{N}{k} k p_{\text{CT}}^{k} (1-p_{\text{CT}})^{N-k} \right. \right. \\ & \left. - \sum_{k=0}^{K-1} \binom{N}{k} k p_{\text{CT}}^{k} (1-p_{\text{CT}})^{N-k} \right] \\ & - N p_{\text{CT}} \left[\sum_{k=0}^{N} \binom{N}{k} p_{\text{CT}}^{k} (1-p_{\text{CT}})^{N-k} \right. \\ & \left. \left. - \sum_{k=0}^{K-1} \binom{N}{k} p_{\text{CT}}^{k} (1-p_{\text{CT}})^{N-k} \right] \right\}. \end{aligned} \tag{37}$$

Using the properties of binomial random variables we have that

$$\sum_{k=0}^{N} \binom{N}{k} k p_{\text{CT}}^{k} (1-p_{\text{CT}})^{N-k} = N p_{\text{CT}}, \tag{38}$$

and

$$\sum_{k=0}^{N} \binom{N}{k} p_{\text{CT}}^{k} (1-p_{\text{CT}})^{N-k} = 1. \tag{39}$$

Now, equation (37) (or equivalently (36)) is equal to

$$\frac{\partial P^{\text{loc}}_{\text{CT}}}{\partial p_{\text{CT}}} = \sum_{k=0}^{K-1} \binom{N}{k} (N p_{\text{CT}} - k) p_{\text{CT}}^{k-1} (1-p_{\text{CT}})^{N-k-1}. \tag{40}$$

It can be observed that (36) is always positive for $p_{\text{CT}} < \frac{K}{N}$, and (40) is always positive for $p_{\text{CT}} > \frac{K}{N}$. As a result $\frac{\partial P^{\text{loc}}_{\text{CT}}}{\partial p_{\text{CT}}}$ is positive for any value of p_{CT}; therefore, $P^{\text{loc}}_{\text{CT}}$ is an increasing function of p_{CT}, and consequently of T_{T}.

Appendix B
Maximum Value of $p_s\lambda$

The first and second derivatives of $p_s\lambda$ w.r.t. λ can be obtained as

$$\frac{\partial p_s\lambda}{\partial \lambda} = \sum_{q=0}^{N} p_{s|q} \frac{x^q e^{-x}}{q!} (q - x + 1), \tag{41}$$

$$\frac{(\partial p_s\lambda)^2}{\partial^2 \lambda} = \sum_{q=0}^{N} p_{s|q} \frac{x^{q-1} e^{-x}}{q!} \left[(q-x)(q-x+1) - x \right], \tag{42}$$

where $x = 2N\lambda T_p$. For $x < 1$ the derivative in (41) is positive, and for $x > N+1$ it is negative. Therefore, $p_s\lambda$ has at least one maximum within $x \in [1, N+1]$. In practical scenarios the value of $p_{s|q}$ for $k > 0$ is usually small, so that it can be approximated by zero. For a special case where $p_{s|q>0} = 0$, (41) is zero if

$x = 1$, and (42) is negative, and as a result $\lambda_{\text{opt}}^{\text{low}} = \frac{1}{2NTp}$ maximizes $P_{\text{CT}}^{\text{loc}}$. This corresponds to a lower bound on the optimal point in a general problem (i.e., $p_{s|q>0} \neq 0$).

APPENDIX C
CRAMÉR RAO LOWER BOUND FOR CTS

The upper bound on the sum operation in (29) for CTS is ∞ (note that in practice at most $\frac{T_{\text{T}}}{T_{\text{p}}}$ packets can be transmitted from an anchor), and this makes the CRB calculation very difficult even if it is implemented numerically. To reduce the complexity of the problem, the observation of a sensor node from the jth anchor is divided into two parts: Either a sensor node does not receive any packet from this anchor (no information is obtained), or it receives one or more packets. Since the anchor and the sensor node do not move very much during the localization procedure, their distance can be assumed almost constant, and therefore the noise power is the same for all measurements obtained from an anchor. When a sensor node gathers multiple measurements contaminated with independent noise with the same power (diagonal covariance matrix), CRB can be computed with less complexity. We will explain complexity reduction for the first anchor, and then generalize for the other anchors.

Considering the first anchor, each element of the FIM can be calculated in two parts: no correct packet reception, and one or more correct packet receptions from this anchor, which can be formulated as

$$\mathbf{I}(\mathbf{x})_{i,j} = P_1^0 \mathbf{I}(\mathbf{x}|q_1 = 0)_{i,j} + P_1^{>0} \mathbf{I}(\mathbf{x}|q_1 > 0)_{i,j}, \tag{43}$$

where P_1^0 is the probability that no packet is received from the first anchor, and $P_1^{>0} = \sum_{q_1=1}^{\infty} P_1^k$ is the probability that one or more than one packets are received from the first anchor which depends on the distance between the sensor node and the anchor. The second term in (43) can be expanded as

$$\begin{aligned}
&\mathbf{I}(\mathbf{x}|q_1 > 0)_{i,j} \\
&= \frac{1}{P^{\text{loc}}} \sum_{q_N=0}^{Q_N} \cdots \sum_{q_2=0}^{Q_2} \\
&\qquad \text{s.t. } \{q_1,\ldots,q_N\} \text{ enable self-localization} \\
&\quad \times \left\{ 1\sigma_1^{-2} \frac{\partial f_1}{\partial x_i} \frac{\partial f_1}{\partial x_j} + c_1 + 1\sigma_1^{-4} \frac{\partial \sigma_1^2}{\partial x_i} \frac{\partial \sigma_1^2}{\partial x_j} + c_2 \right\} \\
&\quad \times P_1^1 / P_1^{>0} \Pi_{j=2}^N P_j^{q_j} \\
&\quad + \left\{ 2\sigma_1^{-2} \frac{\partial f_1}{\partial x_i} \frac{\partial f_1}{\partial x_j} + c_1 + 2\sigma_1^{-4} \frac{\partial \sigma_1^2}{\partial x_i} \frac{\partial \sigma_1^2}{\partial x_j} + c_2 \right\} \\
&\quad \times P_1^2 / P_1^{>0} \Pi_{j=2}^N P_j^{q_j} \\
&\quad + \vdots \\
&\quad \left\{ k\sigma_1^{-2} \frac{\partial f_1}{\partial x_i} \frac{\partial f_1}{\partial x_j} + c_1 + k\sigma_1^{-4} \frac{\partial \sigma_1^2}{\partial x_i} \frac{\partial \sigma_1^2}{\partial x_j} + c_2 \right\} \\
&\quad \times P_1^k / P_1^{>0} \Pi_{j=2}^N P_j^{q_j} \\
&\quad + \vdots
\end{aligned} \tag{44}$$

where c_1 and c_2 are affected only by measurements from the other anchors. Using a simple factorization we have

$$\begin{aligned}
\mathbf{I}(\mathbf{x}|q_1 > 0)_{i,j} = \frac{1}{P^{\text{loc}}} & \sum_{q_N=0}^{Q_N} \cdots \sum_{q_2=0}^{Q_2} \\
& \text{s.t. } \{q_1,\ldots,q_N\} \text{ enable self-localization} \\
& \times \left\{ g_j \left[\sigma_1^{-2} \frac{\partial f_1}{\partial x_i} \frac{\partial f_1}{\partial x_j} \right.\right. \\
& \left.\left. + \sigma_1^{-4} \frac{\partial \sigma_1^2}{\partial x_i} \frac{\partial \sigma_1^2}{\partial x_j} \right] + c_1 + c_2 \right\} \Pi_{j=2}^N P_j^{q_j}
\end{aligned} \tag{45}$$

where

$$g_j = \frac{\sum_{q_j=1}^{\infty} k P_j^k}{\sum_{q_j=1}^{\infty} P_j^k} = \frac{\lambda T_{\text{T}} p_{s|\mathbf{d}}^j}{1 - P_j^0}. \tag{46}$$

Now, we define $\mathbf{a}_{N\times 1}$ with its kth element a_k either zero (if $q_k = 0$) or g_j (if $q_k > 0$). We also define $\mathbf{b}_{N\times 1}$ with its kth element $b_k = [\sigma_k^{-2} \frac{\partial f_k}{\partial x_i} \frac{\partial f_k}{\partial x_j} + \sigma_k^{-4} \frac{\partial \sigma_k^2}{\partial x_i} \frac{\partial \sigma_k^2}{\partial x_j}]$. Then, we have

$$\begin{aligned}
\mathbf{I}(\mathbf{x}|\mathbf{a})_{i,j} = & \frac{1}{P^{\text{loc}}} \\
& \times \left(\mathbf{a}^T \mathbf{b}\right) \left(\Pi_{n=1}^{N-n_{\mathbf{a}}} P_{k,a_k=0}^0 \right) \left(\Pi_{n=1}^{n_{\mathbf{a}}} (1 - P_{k,a_k>0}^0) \right),
\end{aligned} \tag{47}$$

where $n_{\mathbf{a}}$ is the number of non-zero elements in $\mathbf{a}$. Hence, to evaluate $\mathbf{I}(\mathbf{x})_{i,j}$ for the localizable scenarios only $\binom{N}{K}$ possible states (different realizations of $\mathbf{a}$ which lead to localizable scenarios) have to be considered. This number is the same as that of CFS.

REFERENCES

[1] L. Paull, S. Saeedi, M. Seto, and H. Li, "AUV navigation and localization: A review," *IEEE J. Ocean. Eng.*, vol. 39, no. 1, pp. 131–149, Jan. 2013.

[2] S. Chatzicristofis *et al.*, "The NOPTILUS project: Autonomous multi-AUV navigation for exploration of unknown environments," in *Proc. IFAC Workshop NGCUV*, 2012, vol. 3, pp. 373–380.

[3] M. Stojanovic and J. Preisig, "Underwater acoustic communication channels: Propagation models and statistical characterization," *IEEE Commun. Mag.*, vol. 47, no. 1, pp. 84–89, Jan. 2009.

[4] G. Han, J. Jiang, L. Shu, Y. Xu, and F. Wang, "Localization algorithms of underwater wireless sensor networks: A survey," *Sensors*, vol. 12, no. 2, pp. 2026–2061, 2012.

[5] M. Erol-Kantarci, H. T. Mouftah, and S. Oktug, "A survey of architectures and localization techniques for underwater acoustic sensor networks," *IEEE Commun. Surveys Tuts.*, vol. 13, no. 3, pp. 487–502, 3rd Quart. 2011.

[6] H. Jamali-Rad, H. Ramezani, and G. Leus, "Sparsity-aware multi-source RSS localization," *Signal Process.*, vol. 101, pp. 174–191, Aug. 2014.

[7] P. Kuakowski, J. Vales-Alonso, E. Egea-López, W. Ludwin, and J. García-Haro, "Angle-of-arrival localization based on antenna arrays for wireless sensor networks," *Comput. Elect. Eng.*, vol. 36, no. 6, pp. 1181–1186, Nov. 2010.

[8] S. P. Chepuri, G. Leus, and A.-J. van der Veen, "Sparsity-exploiting anchor placement for localization in sensor networks," *arXiv preprint arXiv:1303.4085*, 2013.

[9] R. Stuart, "Acoustic digital spread spectrum: An enabling technology," *Sea Technol.*, vol. 46, no. 10, pp. 15–20, 2005.

[10] X. Cheng, H. Shu, and Q. Liang, "A range-difference based self-positioning scheme for underwater acoustic sensor networks," in *Proc. Int. Conf. WASA*, 2007, pp. 38–43.

[11] A.-K. Othman, "GPS-less localization protocol for underwater acoustic networks," in *Proc. 5th IFIP Int. Conf. WOCN*, 2008, pp. 1–6.

[12] M. K. Watfa, T. Nsouli, M. Al-Ayache, and O. Ayyash, "Reactive localization in underwater wireless sensor networks," in *Proc. 2nd ICCNT*, 2010, pp. 244–248.
[13] S. Shahabudeen, M. Motani, and M. Chitre, "Analysis of a high-performance MAC protocol for underwater acoustic networks," *IEEE J. Ocean. Eng.*, vol. 39, no. 1, pp. 74–89, Jan. 2014.
[14] J.-P. Kim, H.-P. Tan, and H.-S. Cho, "Impact of MAC on localization in large-scale seabed sensor networks," in *Proc. IEEE Int. Conf. AINA*, 2011, pp. 391–396.
[15] A. Syed, W. Ye, and J. Heidemann, "Comparison and evaluation of the T-Lohi MAC for underwater acoustic sensor networks," *IEEE J. Sel. Areas Commun.*, vol. 26, no. 9, pp. 1731–1743, Dec. 2008.
[16] H. Ramezani and G. Leus, "L-MAC: Localization packet scheduling for an underwater acoustic sensor network," in *Proc. IEEE ICC*, 2013, pp. 1459–1463.
[17] H. Ramezani and G. Leus, "DMC-MAC: Dynamic multi-channel MAC in underwater acoustic networks," in *Proc. EUSIPCO*, Marrakech, Morocco, 2013, pp. 1–5.
[18] H. Ramezani and G. Leus, "Ranging in an underwater medium with multiple isogradient sound speed profile layers," *Sensors*, vol. 12, no. 3, pp. 2996–3017, 2012.
[19] R. Cardinali, L. De Nardis, M. Di Benedetto, and P. Lombardo, "UWB ranging accuracy in high and low-data-rate applications," *IEEE Trans. Microw. Theory Tech.*, vol. 54, no. 4, pp. 1865–1875, Jun. 2006.
[20] P. Carroll *et al.*, "On-demand asynchronous localization for underwater sensor networks," *Oceans*, vol. 62, no. 13, pp. 3337–3348, Jul. 2014.
[21] H.-P. Tan, Z. A. Eu, and W. K. Seah, "An enhanced underwater positioning system to support deepwater installations," in *Proc. MTS/IEEE Biloxi-Marine Technol. Future, Global Local Challenges OCEANS*, 2009, pp. 1–8.
[22] F. Fazel, M. Fazel, and M. Stojanovic, "Random access compressed sensing over fading and noisy communication channels," *IEEE Trans. Wireless Commun.*, vol. 12, no. 5, pp. 2114–2125, May 2013.
[23] M. Stojanovic, "On the relationship between capacity and distance in an underwater acoustic communication channel," *SIGMOBILE Mobile Comput. Commun. Rev.*, vol. 11, no. 4, pp. 34–43, Oct. 2007.
[24] H. Jamali-Rad, H. Ramezani, and G. Leus, "Cooperative localization in partially connected mobile wireless sensor networks using geometric link reconstruction," in *Proc. IEEE ICASSP*, 2012, pp. 2633–2636.
[25] *Evologics, Underwater Acoustic Modems, S2CR Series*. [Online]. Available: http://www.evologics.de/en/products/acoustics/s2cr_12_24.html
[26] H. Ramezani, F. Fazel, M. Stojanovic, and G. Leus, "Packet scheduling for underwater acoustic sensor network localization," in *Proc. IEEE ICC*, 2014, pp. 108–113.

Hamid Ramezani (S'11) was born in Tehran, Iran. He received the B.Sc. degree in electrical engineering from Tehran University, Tehran, and the M.Sc. degree in telecommunications engineering from the Iran University of Science and Technology, Tehran, in 2007. He worked at several companies focusing on the implementations of wireless system standards such as DVB-T and DVB-H. He is currently pursuing the Ph.D. degree with the Electrical Engineering Department, Delft University of Technology (TU Delft), Delft, The Netherlands. His current research interests include Underwater acoustic communications and networking.

Fatemeh Fazel (S'05–M'07) received the B.Sc. degree from Sharif University, Tehran, Iran, the M.Sc. degree from University of Southern California, and the Ph.D. degree from the University of California, Irvine, all in electrical engineering. She is currently an Associate Research Scientist in the Electrical and Computer Engineering Department, Northeastern University, Boston, MA, USA. Her research interests are in signal processing methods for wireless communications and sensor networks.

Milica Stojanovic (S'90–M'93–SM'08–F'10) received the B.S. degree from the University of Belgrade, Serbia, in 1988, and the M.S. and Ph.D. degrees in electrical engineering from Northeastern University, Boston, MA, USA, in 1991 and 1993, respectively. She was a Principal Scientist at the Massachusetts Institute of Technology, and in 2008 joined Northeastern University where she is currently a Professor of electrical and computer engineering. She is also a Guest Investigator at the Woods Hole Oceanographic Institution, and a Visiting Scientist at MIT. Her research interests include digital communications theory, statistical signal processing and wireless networks, and their applications to underwater acoustic systems. She is an Associate Editor for the IEEE JOURNAL OF OCEANIC ENGINEERING and a past Associate Editor for the IEEE TRANSACTIONS ON SIGNAL PROCESSING and TRANSACTIONS ON VEHICULAR TECHNOLOGY. She also serves on the Advisory Board of the IEEE Communication Letters, and chairs the IEEE Ocean Engineering Society's Technical Committee for Underwater Communication, Navigation and Positioning.

Geert Leus (M'01–SM'05–F'12) received the M.Sc. and the Ph.D. degrees in applied sciences from the Katholieke Universiteit Leuven, Belgium, in June 1996 and May 2000, respectively. Currently, he is an "Antoni van Leeuwenhoek" Full Professor with the Faculty of Electrical Engineering, Mathematics and Computer Science, Delft University of Technology, The Netherlands. His research interests are in the area of signal processing for communications. He received a 2002 IEEE Signal Processing Society Young Author Best Paper Award and a 2005 IEEE Signal Processing Society Best Paper Award. He was the Chair of the IEEE Signal Processing for Communications and Networking Technical Committee, and an Associate Editor for the IEEE TRANSACTIONS ON SIGNAL PROCESSING, the IEEE TRANSACTIONS ON WIRELESS COMMUNICATIONS, the IEEE SIGNAL PROCESSING LETTERS, and the *EURASIP Journal on Advances in Signal Processing*. Currently, he is a Member-at-Large to the Board of Governors of the IEEE Signal Processing Society and a member of the IEEE Sensor Array and Multichannel Technical Committee. Finally, he serves as the Editor in Chief of the *EURASIP Journal on Advances in Signal Processing*.